J Mater Sci: Mater Med (2009) 20:655–665
DOI 10.1007/s10856-008-3602-3

Estimation of hydrodynamic shear stresses developed on human osteoblasts cultured on Ti–6Al–4V and strained by four point bending. Effects of mechanical loading to specific gene expression

Petros A. Kokkinos · Ioannis K. Zarkadis · Thrassos T. Panidis · Despina D. Deligianni

Received: 21 March 2008 / Accepted: 23 September 2008 / Published online: 21 October 2008

Abstract The aim of the present investigation was to study the effects of mechanical strain on the orthopedic biomaterial Ti–6Al–4V-osteoblast interface, using an in vitro model. Homogeneous strain was applied to Human Bone Marrow derived Osteoblasts (HBMDOs) cultured on Ti–6Al–4V, at levels which are considered physiological, by a four-point bending mechanostimulatory system. A simple model for the estimation of maximum hydrodynamic shear stresses developed on cell culture layer and induced by nutrient medium flow during mechanical loading, as a function of the geometry of the culture plate and the load characteristics, is proposed. Shear stresses were lower than those which can elicit cell response. Mechanical loading was found that contributes to the regulation of osteoblast differentiation by influencing the expression of the osteoblast-specific transcription factor Cbfa1, both at the mRNA and protein level, and also the osteocalcin expression, whereas osteopontin gene expression was unaffected by mechanical loading at all experimental conditions.

P. A. Kokkinos · D. D. Deligianni (✉)
Biomedical Engineering Laboratory, Department of Mechanical Engineering and Aeronautics, University of Patras, Rion, 26500 Patra, Greece
e-mail: deligian@mech.upatras.gr
URL: http://www.mech.upatras.gr/~deligian/

I. K. Zarkadis
Department of Biology, School of Medicine, University of Patras, Rion, 26500 Patra, Greece

T. T. Panidis
Laboratory of Applied Thermodynamics (LAT), Department of Mechanical Engineering and Aeronautics, University of Patras, Rion, 26500 Patra, Greece

1 Introduction

All cells experience and respond to intracellular and extracellular mechanical stimuli [1, 2]. In response to these stimuli they are modifying their rate of division, death, differentiation, movement, signal transduction, gene expression, secretion, and endocytosis [2, 3]. Mechanical signals play an essential role in both normal and pathological development of a variety of tissue types, including bone [4]. The capacity of bone tissue to alter its mass and structure in response to mechanical demands has long been recognized [5].

In vitro studies led to the conclusion that the response of mechanically stimulated osteoblasts depends on strain kind, magnitude, frequency and time course. Several studies indicate that osteoblastic cells respond to physical loading by transducing signals that alter gene expression patterns. In specific, Core-binding factor alpha 1 (Cbfa1) mRNA has been found to increase dramatically in osteoblastic cells after 0.5 h of continuously applied mechanical stretching [6]. Mechanical loading of osteoblasts or osteoblast-like cells has generally shown controversary results regarding osteocalcin (OC) gene expression and protein synthesis [7–11]. Studies from different research groups have confirmed that the osteopontin (OPN) gene expression is unaffected by longitudinal strain but is very sensitive to oscillating fluid flow [12–15].

Cellular responses are also material dependent, demonstrating that the substrate material has a definitive influence on cell behaviour [16, 17]. The strong influence of the solid microenvironment on bone cell behaviour and function complicates the study of bone cell mechanotransduction mechanisms. Osteoblasts attached on different surfaces express variable responses to mechanical stimulation. Human osteoblasts or osteoblast-like cells cultured on

bioceramics covered Ti–6Al–4V and subjected to mechanical strains have shown different responses in terms of morphology, DNA synthesis, lactate dehydrogenase (LDH) release, alkaline phosphatase (ALP) activity, osteocalcin, collagen and total protein synthesis, in relationship with the ceramic coating [18, 19].

Moreover, mechanical stress has to be taken into account in the osseointegration process of orthopedic and dental implants, since their implantation in the host bone assumes that they will be subjected to mechanical loading [18]. Understanding the mechanisms of load transduction at the tissue/implant interface and the conversion of mechanical information into biochemical responses by osteoblasts, will provide new insights in elucidating the role of mechanical loading in the osseointegration process of bone implants. Numerous studies examining the in vitro cellular response to strain have included a variety of mechanisms to produce strain [20, 21]. Cell loading systems, based on the four-point bending principle, result in homogeneous strain application to the whole cell population [22–25]. However, when dynamic rather than static inputs are involved in culture mechanostimulation experiments, motion of the substrate induces motion of the overlying liquid nutrient medium. In turn, motions of the nutrient medium occur in association with two categories of dynamic fluid stresses: shear stresses arising in concert with fluid velocity gradients, and normal stresses arising in concert with fluid pressure and acceleration. The reactive fluid stresses, developed upon the culture layer in mechanostimulation experiments, may seriously confound data interpretation depending on the specifics of experimental parameters and study design. Thus, the characterization of the nature of these reactive fluid stresses is necessary. Brown et al. [26] developed computer models for the calculation of nutrient medium flow fields for two cell culture mechanostimulatory systems.

Mechanical loading of cells in vitro has proven to be a very useful tool in understanding the underlying mechanisms of load transduction at the tissue/implant interface [16]. The selection of the cell culture model, the loading conditions, the cell culture substrate and the mechanostimulatory system used in this kind of studies are very important factors for the significance of the experimental data from the clinical point of view. Moreover, the characterization of the mechanical loading system is mandatory since strain and/or fluid movement may activate different signalling pathways.

The aim of the present study was to investigate the effects of mechanical strain on the orthopedic biomaterial Ti–6Al–4V/osteoblast interface in terms of differentiation marker genes expression, shortly after the application of mechanical stimuli, at small deformations and frequencies of the daily living activities. Gene expression of the osteoblast-specific transcription factor Cbfa1, the most osteoblast-specific gene osteocalcin, and the fluid-shear sensitive gene osteopontin have been studied, as function of strain frequency, magnitude and time interval. Homogeneous strain has been applied by a custom made device, based on the four-point bending principle, to HBMDOs cultured on Ti–6Al–4V, at levels which are measured experimentally on the external surface of bones and are regarded as physiological, and on the basis of estimated deformation on hip stem prostheses [19, 27–29]. In order to characterize the nutrient medium flow field during straining, a simple model for the estimation of maximum hydrodynamic shear stresses developed in culture cells strained in the four point bending device, as a function of the geometry of the culture plate and the load characteristics, is proposed.

2 Materials and methods

2.1 Biomaterial

A sheet of Ti–6Al–4V was obtained by TIMET (Savoie S. A., France) (Fig. 1, TAV). The titanium alloy had the following composition based on the manufacturer's heat chemical analysis (wt.%): Fe 0.127, V 3.927, Al 6.107, C 0.023, O 0.168, N 0.005. Mean mechanical properties were as follows: 0.2% yield stress (MPa): 947, ultimate tensile strength (MPa): 1043, elongation of 50 mm (%): 19.

2.2 Ti–6Al–4V surface preparations

The surface of Ti–6Al–4V was first wet-ground through 1200 grit silicon carbide (SiC) abrasive paper, degreased in acetone and rinsed with double distilled water (ddH_2O). It was further cleaned in 50% phosphoric acid for 30 min, and rinsed again with ddH_2O. The surface was passivated with nitric acid, at room temperature, for 20 min and after this step it was thoroughly rinsed in ddH_2O and air dried [30, 31].

To create cell culture wells on the biomaterial's surface, conventional tissue culture dishes (greiner bio-one, cellstar, 60/15 mm) have been used. The bottom of the dishes was removed with a hot blade and the resulted plastic rings were attached on the Ti–6Al–4V surface using a silicone adhesive (Silicone Rubber Adhesive Sealant, GE Silicones, Holland) (Fig. 1, S, C). The silicone was allowed to cure at ambient conditions for 72 h and the surface was sterilized with 100% ethanol, air-dried into a laminar flow cell culture hood, exposed under ultraviolet light for 24 h and conditioned with α-MEM in a cell culture incubator until use [22].

Fig. 1 Photograph of the mechanostimulatory cell culture system used in this study into a cell culture incubator. The device was composed of an aluminum alloy base (a), two arched bars (b), a frame (c), a cam (d) and an electrical motor (e). The Ti–6Al–4V plate (TAV, C), shown under the strain device, was prepared in the exact same manner as the one used in the device (TAV, S) and was the non-strained control. A near uniform surface strain field was generated across the inner span of the bended Ti–6Al–4V foil

2.3 Cell culture

Human bone marrow stromal cells (hMSCs) which were obtained by aspiration from the femoral diaphysis of patients undergoing total hip replacement surgery were used in this study. From each donor, a single-cell suspension was prepared by repeatedly aspirating the cells successively through 19 and 21-gauge needles. To induce osteogenic differentiation, cells were cultured in alpha-Minimal Essential Medium (α-MEM, Biochrom KG, seromed, Berlin), with 10% fetal bovine serum (FBS, Biochrom), supplemented with 2.5 μg/ml amphotericin B (Biochrom), 50 μg/ml gentamycin (Biochrom), $10-8$ M dexamethasone (Sigma Aldrich), 1.5 mM β-glycerophosphate (Sigma) and 50 μg/ml ascorbic acid (Sigma) The cells were incubated under a humidified 5% CO_2/air atmosphere at 37°C until confluent, detached by incubation with 0.25% trypsin (Biochrom) and passaged. Medium was changed every 3 days. Before the seeding of the osteoblasts on the cell culture wells, created on the Ti–6Al–4V surface, the osteoblastic differentiation was checked by staining for alkaline phosphatase activity (ALP), and calcification, using histochemical methods [32]. Cells of the second to the fourth passage were used for the experiments, seeded at a concentration of 10^5 cells/cm^2 on the biomaterial and allowed to attach for 72 h before the application of strain. Cell cultures were tested periodically and found to be mycoplasma-free.

2.4 Mechanical stimulation

The cell-loading system used in this study applies four-point bending on a sheet of Ti–6Al–4V (Fig. 1, TAV). The device is composed of an aluminum alloy base (Fig. 1a), two arched bars (Fig. 1b) and a frame (Fig. 1c), a cam (Fig. 1d) and an electrical motor (Fig. 1e). The Ti–6Al–4V sheet with the culture wells rests on the two arched bars and is loosely screwed with four pins to the frame which is connected to a cam. The cam is connected to an electrical motor (AC/DC current gear motor) which in turn is connected to an adjustable voltage regulator unit. HBMDOs were subjected to two different strain magnitudes (500, 1000 με), at frequencies of load application of 0.5 and 1 Hz, for time periods of 1.5, 3 and 6 h.

2.5 Characterization of the strain device

2.5.1 Characterization of the strain loading profiles

Strain loading profiles have been determined by uniaxial strain gages (KFG-10-120-C1-11L1M2R, KYOWA, Japan, 10 mm length, 119.6 ± 0.4 Ω resistance and 2.11 ± 1.0% gage factor) mounted on the biomaterial sheet (Fig. 2b). The strain gages were connected to a KYOWA quarter bridge amplifier. The analogue signal output was converted to a digital signal, through an A/D card (KYOWA data logging system UCAM-10A) (Fig. 2a).

2.5.2 Estimation of nutrient fluid flow induced shear stress in culture wells

The derivation of the model for the estimation of maximum hydrodynamic shear stress in culture wells strained in a four-point bending device is based on the assumption (supported by experimental observations) that the fluid free surface remains at all times flat and horizontal, in agreement with the assumption of negligible inertial forces used in previous estimations [33]. Fluid circulation is the result of internal fluid movements, which balance hydrostatic pressure changes due to substrate deformation. Maximum shear is observed at locations half a radius away from the well centre in the long direction of the oscillating plate, where a sinusoidal oscillating flow is established, with cross sectional average velocity:

$$U_{x\ average} = \frac{3r\pi\delta_{max}f\ \sin(2\pi ft)}{32h_0}$$

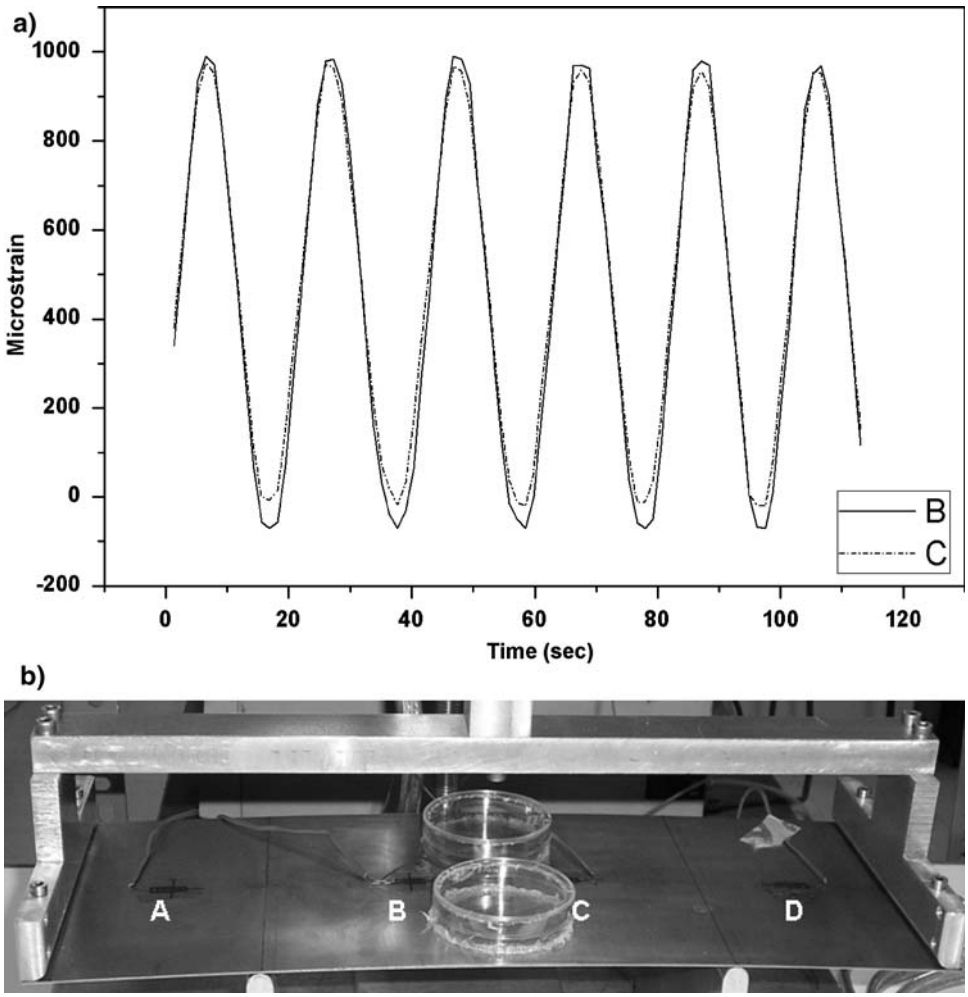

Fig. 2 **a** Typical strain versus time profile. Data collected from uniaxial strain gages at the highest strain level used in this study (1000 με) display a sinusoidal wave form and represent positive tensile strains. **b** Image of four strain gages (A, B, C, D) mounted on the top surface of the Ti–6Al–4V sheet

where r is the culture well radius, δ_{max} the maximum deflection at cell wells' edge, f the loading application frequency and h_0 the well filling depth.

Using this as the forcing velocity in the oscillating wall problem (second Stokes problem [34]) the maximum shear stress is obtained as (see appendix)

$$\tau_{0,max} = 0.1326 \frac{\rho\sqrt{\nu} r \delta_{lmax} (\pi f)^{3/2}}{h_0}$$

where ν is the kinematic viscosity and ρ the density of the fluid (Fig. 3).

2.6 Gene expression analysis by semi-quantitative RT-PCR

Total RNA was extracted from osteoblasts after mechanical loading at the strain magnitude of 500 or 1000 με, at 0.5 or 1 Hz, after 1.5, 3 and 6 h, using the Total RNA Isolation NucleoSpin RNA II kit (Macherey-Nagel, Germany). About 150 ng of total RNA from each control and loaded culture were used as a template for reverse transcription.

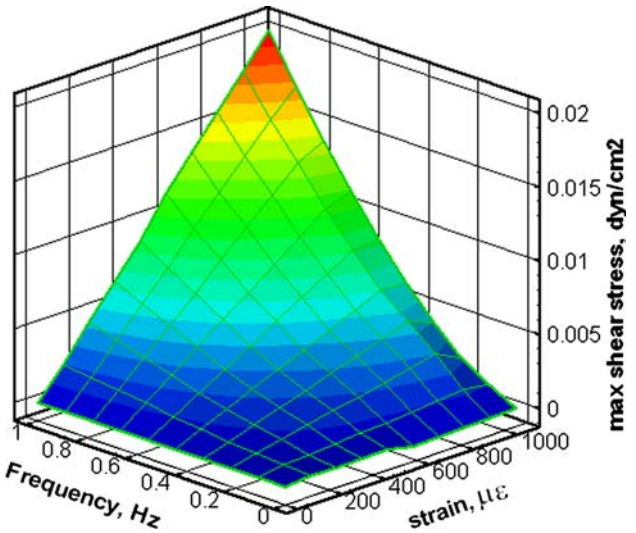

Fig. 3 The calculated maximum shear stress developed in a circular culture well with d = 60 mm placed on the Ti–6Al–4V sheet, and subjected to four-point bending as a function of load application frequency and strain

RT-PCR reactions were carried out using the OneStep RT-PCR kit (QIAGEN). Specific oligonucleotide primers were designed by PC-Gene and OLIGO software, and obtained from the MWG-Biotech AG (Germany). The oligonucleotide sequences were the following: Cbfa1F1: 5′-TGTA GATCCGAGCACCAGCC-3′, Cbfa1R1: 5′-CTTACCTT-GAAGGCCACGGG-3′, OCF1: 5′-ATGAGAGCCCTCAC ACTCCTC-3′, OCR1: 5′-CTAGACCGGGCCGTAGAA GCG-3′, OPNF1: 5′-CCAAGTAAGTCCAACGAAAG-3′, OPNR1: 5′-GGTGATGTCCTCGTCTGTA-3′, GAPDHF1: 5′-CTGCACCACCAACTGCTTAGC-3′, GAPDHR1: 5′-AAGTCAGAGGAGACCACCTGG-3′. The primers for GAPDH were designed on different exons. Amplification was carried out in a thermocycler (Peltier PTC-200) for the optimal number of 33 cycles. The program of the thermal cycler was as follows: 50°C for 30 min, 95°C for 15 min, followed by a 3-step cycling with denaturation at 95°C, annealing, and extension at 72°C. Specific conditions for the studied genes were as follows: Cbfa1: 35 s, 60°C, OC: 30 s, 58°C, OPN: 30 s, 50°C, GAPDH: 45 s, 57°C. After completion of the RT-PCR, samples were analyzed on 2.5% agarose-ethidium bromide gels and visualized under ultraviolet illumination (Figs. 4 and 5). The densitometric value of the RT-PCR product detected with ethidium bromide was determined using Kodak Electrophoresis Documentation and Analysis System (EDAS) 120 (Kodak Digital Science). The reproducibility of the sqRT-PCR experiments was confirmed by repeating each reaction 3 times. Changes in band densitometry were quantified and expressed as percentage relative to the static controls (100%) after normalization with GAPDH expression, according to the formula presented by Di Palma et al. [19]. The percentages quoted are average changes (±SD) of three independent experiments and are summarized graphically (Figs. 6 and 7).

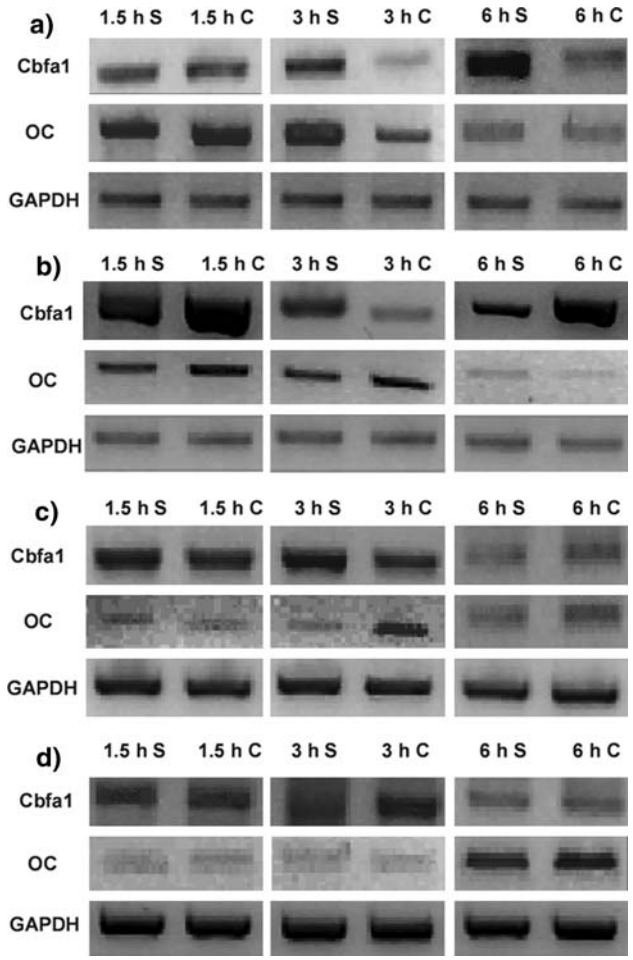

Fig. 4 Semi-quantitative RT-PCR analysis of mRNA expression of Cbfa1 and OC genes. Effects of mechanical loading on the mRNA expression of Cbfa1 and OC in HBMDOs cultured for 1.5, 3 and 6 h on a Ti–6Al–4V substrate as assessed by sqRT-PCR. GAPDH mRNA amplification was included as an internal control and as a measure of RNA integrity. Representative image of sqRT-PCR products visualized under UV light after electrophoresis in a 2.5% agarose ethidium bromide gel. The frequency of the mechanical loading and the strain magnitude was **a** 0.5 Hz, 500 με, **b** 0.5 Hz, 1000 με, **c** 1 Hz, 500 με, **d** 1 Hz, 1000 με. Each experiment was run in triplicate. Strained (S) and unstrained (C) cultures were performed in parallel

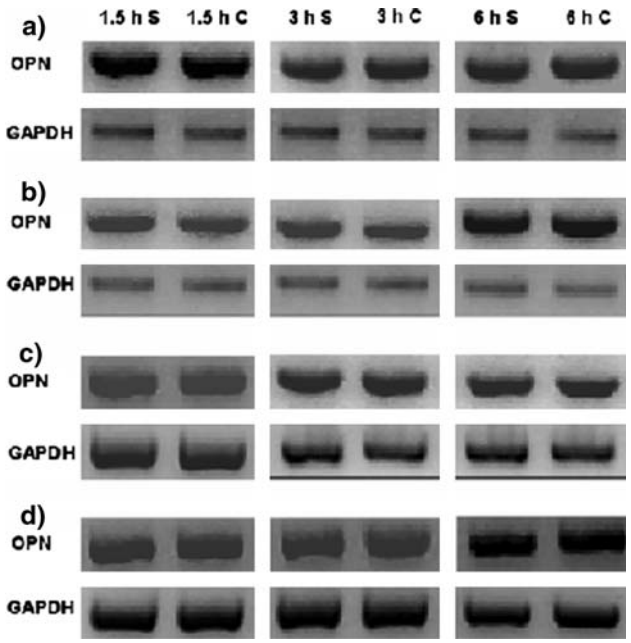

Fig. 5 Semi-quantitative RT-PCR analysis of OPN mRNA expression. Effects of mechanical loading on the OPN mRNA expression in HBMDOs cultured for 1.5, 3 and 6 h on a Ti–6Al–4V substrate as assessed by sqRT-PCR. GAPDH mRNA amplification was included as an internal control and as a measure of RNA integrity. Representative image of sqRT-PCR products visualized under UV light after electrophoresis in a 2.5% agarose ethidium bromide gel. The frequency of the mechanical loading and the strain magnitude was **a** 0.5 Hz, 500 με, **b** 0.5 Hz, 1000 με, **c** 1 Hz, 500 με, **d** 1 Hz, 1000 με. Each experiment was run in triplicate. Strained (S) and unstrained (C) cultures were performed in parallel

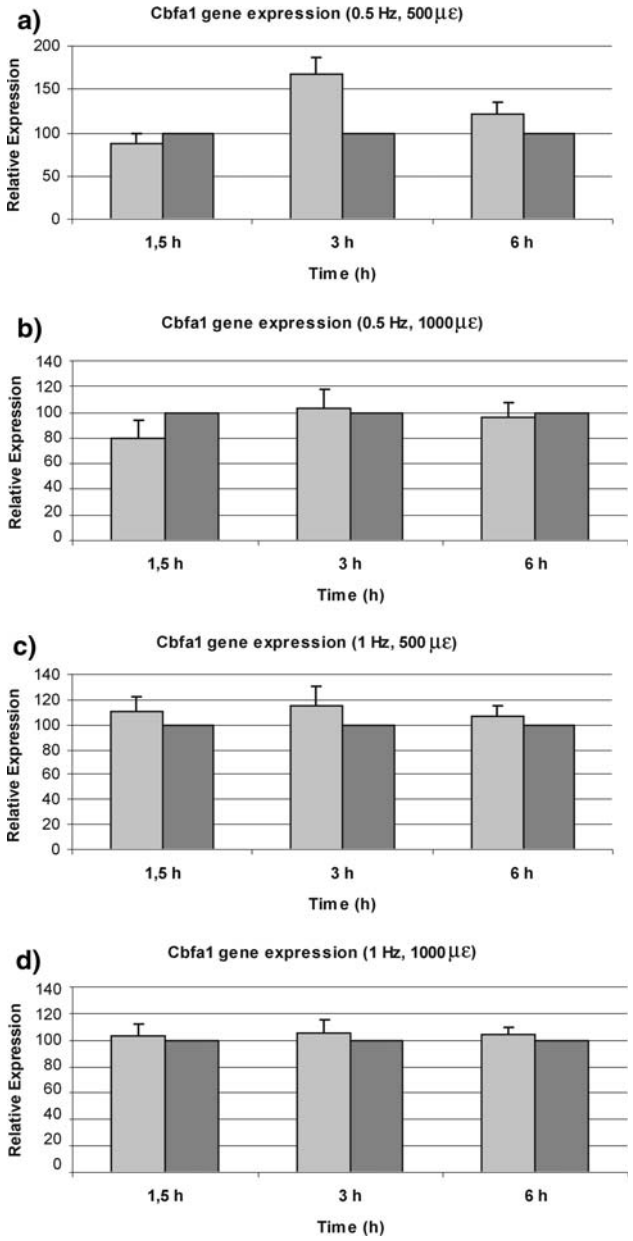

Fig. 6 Semi-quantitative RT-PCR analysis of mRNA expression of Cbfa1 gene. Band densitometry was quantified for Cbfa1 and GAPDH. Diagrams **a**–**d** show the relative Cbfa1 gene expression of the strained osteoblasts (gray columns ■) (% of their respective 100% unstrained controls (black gray columns ■)) after normalization of the bands based on GAPDH internal control expression, according to the formula presented by Di Palma et al. [19]. Data were collected from three independent experiments and the mean values with SDs are presented. **a** 0.5 Hz, 500 με, **b** 0.5 Hz, 1000 με, **c** 1 Hz, 500 με, **d** 1 Hz, 1000 με

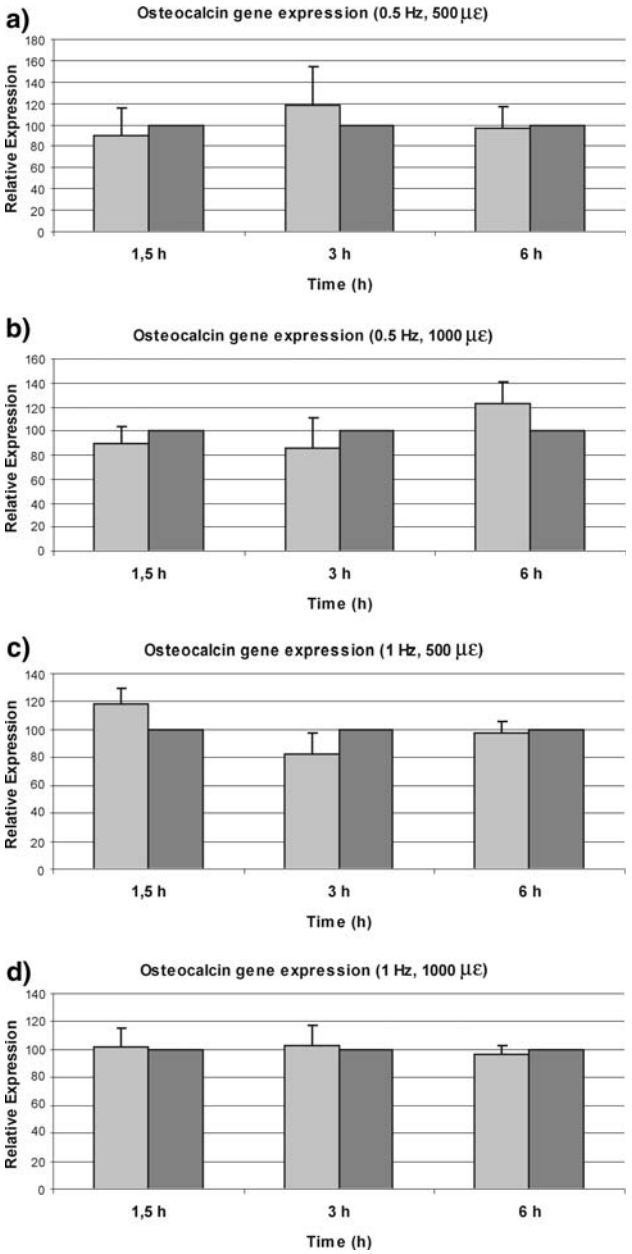

Fig. 7 Semi-quantitative RT-PCR analysis of mRNA expression of OC gene. Band densitometry was quantified for OC and GAPDH. Diagrams **a**–**d** show the relative osteocalcin gene expression of the strained osteoblasts (gray columns ■) (% of their respective 100% unstrained controls (black gray columns ■)) after normalization of the bands based on GAPDH internal control expression, according to the formula presented by Di Palma et al. [19]. Data were collected from three independent experiments and the mean values with SDs are presented. **a** 0.5 Hz, 500 με, **b** 0.5 Hz, 1000 με, **c** 1 Hz, 500 με, **d** 1 Hz, 1000 με

3 Results

3.1 Characterization of strain loading profiles

The cell loading system used in the present study permitted the application of well-characterized cyclic strain to HBMDOs cultured on Ti–6Al–4V. Typical strain versus time profile of maximum deflection of the Ti–6Al–4V sheet (1000 με) is shown in Fig. 2a. Measurements were collected from uniaxial strain gages mounted on the top surface of the biomaterial during cyclic loading (Fig. 2b).

The data show a sinusoidal wave form and represent positive tensile strains. Differences smaller than 10% in strain values obtained from the two strain gages in the homogeneous strain area were observed (Fig. 2a).

3.2 Nutrient flow induced shear stresses

Figure 3 displays the calculated maximum shear stress developed in a circular culture well with d = 60 mm, placed on the Ti–6Al–4V sheet (as it is shown in Fig. 1), and subjected to four-point bending as a function of load application frequency and strain. The maximum stress increases quickly with increasing strain and frequency. The peak shear stress value was estimated as 0.019 dyn/cm^2 and it was observed at locations half a radius away from the centre of the cell culture well in the long direction of the oscillating plate, for strain magnitude of 1000 με and frequency 1 Hz.

3.3 Expression of Cbfa1, osteocalcin and osteopontin genes

The mRNA expression of Cbfa1, osteocalcin and osteopontin genes has been studied by sqRT-PCR for the maximum time interval of 6 h. The DNA amplification products of Cbfa1 (375 bp), OC (303 bp), and OPN (347 bp) were analyzed and normalized to the expression of the housekeeping gene glyceraldehyde-3-phosphate dehydrogenase, GAPDH (405 bp).

It has been observed that the most stimulating condition for Cbfa1 mRNA expression was that of 0.5 Hz, 500 με, 3 h (Figs. 4a and 6a). Mechanical loading at 500 με seems to have a more profound effect on Cbfa1 mRNA expression compared to the higher mechanical stimulation at 1000 με (Figs. 4a–d and 6a–d).

Interestingly, it has been shown that the highest level for osteocalcin mRNA expression was achieved at 0.5 Hz, 500 με, 3 h, corresponding to the higher expression level of Cbfa1 (Figs. 4a and 7a).

Finally, osteopontin gene expression was unaffected by mechanical loading at all experimental conditions (Fig. 5).

4 Discussion

The environment of the prosthetic materials is dynamic after implantation and mechanical deformations at the cell-implant interface have to be considered in understanding and predicting the short- and long-term integration of bone-replacing implants. Numerous studies examining the in vitro cellular responses to strain have been performed, using a variety of mechanisms to produce strain. On the contrary, very few works have studied the response of cells growing on substrates which are typical for orthopedic prosthesis. Cellular responses are material dependent and it has been shown that the substrate material has a definite influence on cell behaviour [17, 18, 35]. Ti–6Al–4V is the biomaterial of choice for the construction of hip implants. Osteoblastic cells grown on Ti–6Al–4V, under cyclic strain, at physiological levels have been found that increased their proliferation and total protein synthesis, whereas alkaline phosphatase activity and osteocalcin concentration were decreased [22, 36]. Opposite results have been found by Di Palma et al. [35]. Mechanical straining at 600 με and 0.25 Hz, of osteoblast-like cells on Ti–6Al–4V, stimulated alkaline phosphatase activity by 25–30%, but had no effect on cell growth. In the present investigation the pattern of gene expression for Cbfa1, OC and OPN has been studied by sqRT-PCR, in HBMDOs growing on the major orthopedic alloy of titanium, Ti–6Al–4V, shortly after the application of mechanical strain, at physiological levels, for the maximum time interval of 6 h.

Typical strains measured on the surface of human tibial bone in vivo during vigorous activity were up to 2,000 microstrain (με) or 0.2% deformation and they can be considered as physiological [37]. The lower levels of the considered as physiological range of strain were used in this study. Frequencies of 0.5 and 1 Hz have been applied as they are considered dominant frequencies of activities of daily living [38, 39].

In this work, the bone marrow donors have undergone total hip replacement. Thus, the use of osteoblasts of primary cultures ensured that the cell-biomaterial interaction was assessed using the cells which will react in vivo with the prosthesis. Many studies use cell culture systems of non-human origin, tumor cell lines or they exploit cells which are not opposed to orthopedic implants in situ.

The use of the four point bending principle for the design and construction of the mechanostimulatory cell culture system permitted the homogeneous application of characterized cyclic strains to the whole population of osteoblastic cells. Variations observed in measured strain values from strain gages mounted on symmetric positions on the top of the Ti–6Al–4V surface were attributed to the subtle mispositioning of the plate on the arched bars, the pins which connect the Ti–6Al–4V sheet to the aluminum frame and the cam, the alignment of the strain gages, and the subtle variations in the thickness of the plate [22] (Fig. 2a).

Cbfa1 can directly stimulate transcription of osteoblast-related genes such as those encoding osteocalcin, type I collagen, osteopontin and collagenase 3 [40] and is considered a focal point for integration of a variety of signals affecting osteoblast activity [41]. These signals include information about the extracellular matrix environment as detected through integrin-extracellular matrix (ECM)

interactions and hormone/growth/differentiation factor levels in the extracellular milieu. It has been shown that low level stretching of human osteoblastic cells or stromal cell lines directly up-regulates the expression and DNA binding activity of Cbfa1, providing a molecular link between mechanostressing and stimulation of osteoblast differentiation [6, 40, 41]. This up-regulation of Cbfa1 mRNA was followed by an increase in Cbfa1 protein [6]. No change in the mRNA levels of Cbfa1 has been observed after the stimulation of marrow stromal cells (MSCs) with oscillating fluid flow [13]. It should be noticed that all of these studies use either non-physiologic levels of strain, cell culture substrates of non-orthopedic materials, cell lines, or they study late responses of mechanical strain.

In the present investigation it has been observed that the most stimulating condition for Cbfa1 mRNA expression was that of 0.5 Hz, 500 με, 3 h (Figs. 4a and 6a). Mechanical loading at 500 με seems to have a more profound effect on Cbfa1 mRNA expression compared to the higher mechanical stimulation at 1000 με (Figs. 4a–d and 6a–d). This is in accordance with previous studies and our finding (data not shown) that osteoblastic cells which receive the most intense stretching (1 Hz and 1000 με) secrete the lowest stimulatory activity [22, 24, 42, 43].

The osteocalcin gene is the only truly osteoblast-specific gene, expressed only by fully differentiated osteoblasts [44]. Dynamic mechanical stretching of osteoblasts or osteoblast-like cells on silicone substrates, at physiological strain levels, generally resulted in increased osteocalcin gene expression and protein synthesis [7–11, 45] with some exceptions being reported [42]. Osteoblasts cultured on orthopedic biomaterials display differentiated response when strained. Osteocalcin secretion was not affected by mechanical strain of osteoblasts on alumina-coated titanium alloy [19]. In the present investigation, sqRT-PCR analysis showed that osteocalcin gene expression increased at 0.5 Hz, 500 με, 3 h, in correspondence to the higher expression level of Cbfa1 (Figs. 4a and 7a). On the contrary, Lewandowska-Szumiel et al. [36] found that osteocalcin concentration was significantly decreased in osteoblasts cultured on Ti–6Al–4V substrate and subjected to cyclic elastic strain of 1000 με. The loading frequency in this latter work was 11 Hz. Mechanical loading, by four point bending, with the system used in our study at 11 Hz has been calculated to induce shear stresses by the nutrient medium fluid flow 36 times higher than those induced by mechanical loading of 1 Hz for the same strain (1000 με). This finding suggests that the contribution of shear stress to the cellular responses observed in that study, compared to that of stretch, was much more significant. Given that the cell response is proportional to shear stress [46], the decreased osteocalcin concentration might be due to shear stress rather than to stretch. This was supported by the nitric oxide secretion in the culture which was subjected to straining but not in the control culture. It was also consistent with the findings of Bannister et al. [47], that after 1 h of exposure to shear, osteocalcin levels were reduced in culture.

It has been reported that Cbfa1 does not up regulate osteocalcin gene expression at early stages but does so at a late stage of osteoblast differentiation in vivo and in vitro [40, 48]. In the present investigation, sqRT-PCR analysis showed that osteocalcin gene expression increased at 0.5 Hz, 500 με, 3 h, in correspondence to the higher expression level of Cbfa1 (Figs. 4a and 7a).

Studies from many different research groups have confirmed that osteopontin expression increases at supra-physiological substrate strain (higher than 3000 με) and it is very sensitive to fluid shear [7, 12, 49–52]. Osteopontin exerts various physiologically and pathologically important functions in vitro and in vivo: cell adhesion, migration, survival, angiogenesis, tumorigenesis, metastasis, immune responses, wound healing, host defence, and inhibition of complement-mediated cell lysis [53]. No change in osteopontin mRNA level in response to 0.5% strain at 1 Hz has been observed. In contrast, oscillating fluid flow predicted to occur in the lacunar-canalicular system due to routine physical activities (2 N/m^2, 1 Hz) caused significant increases in both intracellular Ca^{2+} and osteopontin mRNA [12, 54]. The current study showed that osteopontin gene expression was unaffected by mechanical loading at all experimental conditions confirming the above results that fluid forces and not mechanical stretch influence OPN expression in osteoblasts (Fig. 5).

Cyclic bending of the Ti–6Al–4V foil results in cell culture medium movement over the cellular layer. Experimental findings have confirmed, in human bone cells, that strain applied through the substrate and fluid flow stimulate the release of signalling molecules to varying extents. These two types of stimuli, substrate deformation and shear stress, do not affect identically the cell behaviour on rigid biomaterials [35]. Osteopontin gene expression is a marker of fluid shear stress presence, which may dramatically affect the cellular responses. In the current investigation the finding that osteopontin gene expression remains unaltered supports the idea that fluid shear due to the movement of culture medium is insignificant under the loading experimental conditions.

In the mechanostimulatory system used in this study, the generated fluid flow of the nutrient medium, during bending of the Ti–6Al–4V plate, creates shear stresses on the cell culture layer which are maximum at locations half a radius away from the cell well centre in the long direction of the oscillating plate. Although the tensile strain of the culture substrate is almost uniform irrespective of the position of the cell culture well in the region between the loading points (Fig. 1b), the flow velocity at each point on

the Ti–6Al–4V depends on its displacement and the frequency of loading application or strain rate. The maximum hydrodynamic shear stress developed in cell culture wells, strained in a four point bending device, was estimated as a function of the geometry of the culture well and the load characteristics. For the maximum frequency and strain magnitude of this study (1000 με, 1 Hz), the peak shear was calculated to be 0.019 dynes/cm^2. The most stimulating experimental conditions for Cbfa1 and osteocalcin gene expression (500 με and 0.5 Hz), induce shear stress of 0.0033 dynes/cm^2. This value is 10-fold lower than the values of shear stress that have been found experimentally to elicit osteoblastic responses [46, 55, 56]. Most of the studies investigating the effects of shear stress on cells have focused on stress levels somewhat higher than 0.02 dynes/cm^2; therefore, it can be concluded that fluid flow did not contributed to the observed responses, in the present study. Interest in the response of cells to mechanical stimuli has led to the introduction of a variety of laboratory devices designed to deliver quantified mechanical inputs to culture systems. Such devices commonly rely upon distention of a flexible culture substrate. The substrate distention in such systems typically induces motions in the overlying liquid nutrient medium, which in turn exert unintended reactive stresses, mostly shear stresses. The information on the shear stresses is rather limited and relies either on numerical simulations of cell culture mechanostimulus systems with specific characteristics [26] or on rough estimates [33]. It has been shown that the shear stress field shows markedly different characteristics depending on the configuration of the loading system [26]. Thus, in considering whether the role of fluid flow is relevant, each loading system should be studied separately.

The transformation mechanisms, converting the physical stimulus into the cellular response, called mechanotransduction, are not well known. Certainly, it is clear that mechanical signals in bone alter its transcriptional activity, and this is an effective strategy for a "smart" material to accommodate new loading challenges. Critical components in the load profile for the high responsiveness of bone cells to mechanical stimuli, are still unclear. Virtually, every type of signalling cascade is subject to activation by mechanical forces. Moreover, the promoter of several osteoblast phenotypic genes including osteopontin and osteocalcin, is responsive to a number of different transcription factors. This could justify the different profile of gene expression presented in the current study for osteocalcin and osteopontin.

Further work is being carried out to determine the long term effects of cyclic mechanical stretching, and to define the signalling biochemical pathways involved in the mechanotransduction process, using the presented experimental model.

5 Conclusions

In conclusion, our experiments demonstrated that HBMDOs growing on Ti–6Al–4V implant surface translate the mechanical information after mechanical loading at physiological levels into an adaptive response in terms of differentiation and production of extracellular matrix components, by influencing the level of bone-related genes (osteocalcin) and transcription factors (Cbfa1). The theoretical analysis of the predicted fluid flow induced shear stress in the used mechanostimulatory system showed that fluid shear due to the movement of culture medium is insignificant under the loading experimental conditions. The fluid shear sensitive osteopontin gene expression was unaffected by mechanical loading at all experimental conditions confirming the above mentioned finding.

Acknowledgements This project was financially supported by the project, "K. Karatheodori" (2992) of the Research Committee of the University of Patras. The authors wish to express their gratitude to Dr. P. Korovessis, for providing bone marrow.

Appendix: Maximum shear stress estimation

In the following a simple model for the estimation of maximum hydrodynamic shear stress in culture wells with substrates strained by a four point bending devise, is obtained. The derivation is based on the assumption (supported by experimental observations) that the fluid free surface remains at all times flat and horizontal, in agreement with the assumption of negligible inertial forces used in previous estimations [33]. Fluid circulation is the result of internal fluid movements, which balance hydrostatic pressure changes due to substrate deformation.

The geometry of the experimental apparatus and the corresponding parameters are defined in the following figure. The culture well may be cylindrical in shape (of radius l, centered at $y = 0$, $z = 0$) or rectangular (of half length l and width w, with primary axes along the y and z axes). The well is filled with liquid to a height h_0.

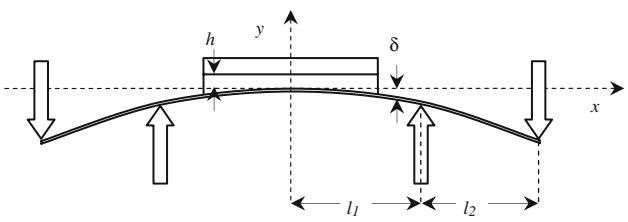

The volume of the liquid in the well is constant and at any time during the forcing cycle is given by the equation

$$V = h_0 \int_{-l}^{l} w(x)dx = \int_{-l}^{l} [h(t) + \delta(t)]w(x)dx$$

with $w = \sqrt{l^2 - x^2}$ for a cylindrical well.

Based on four point bending kinematics the surface of the substrate, in the area between the two inner supports, follows the shape of a parabola with deflection

$$\delta = Cx^2, \quad |x| \le l_1$$

With a sinusoidal forcing the deflection corresponding to the well wall a $x = l$ is

$$\delta_l = \delta_{lmax} \frac{(1 - \cos(2\pi ft))}{2}$$

where δ_{lmax} is the maximum deflection at the well wall and f the frequency of the forcing.

Thus, within the well boundaries, δ as a function of δ_{lmax} is

$$\delta(x,t) = \frac{\delta_{lmax}}{2} \frac{x^2}{l^2} (1 - \cos(2\pi ft))$$

Assuming that the surface of the liquid in the well remains flat and horizontal during the forcing cycles it can be shown that the minimum depth (corresponding to $x = 0$) follows the relation

$$h = h_0 - \frac{\delta_{lmax}}{\eta} (1 - \cos(2\pi ft))$$

where η is a shape factor taking values 3 for a rectangular well and 8 for a cylindrical one.

The total depth at each position, x, changes with time during the forcing cycle as

$$\frac{dH}{dt} = \frac{d(h+\delta)}{dt} = \left(\frac{1}{\eta} - \frac{x^2}{2l^2}\right) \delta_{lmax} \frac{d\cos(2\pi ft)}{dt}$$
$$= -\left(\frac{2}{\eta} - \frac{x^2}{l^2}\right) \delta_{lmax} \pi f \sin(2\pi ft)$$

It follows that for $\frac{2}{\eta} - \frac{x^2}{l^2} = 0$, that is at locations $x_p = \pm\frac{1}{2}l$ for the cylindrical well and $x_p = \pm\sqrt{\frac{2}{3}}l$ for the rectangular one the total liquid depth remains constant through the cycle with $H = h_0$.

The liquid flows through any constant x cross section to balance the pressure and maintain the flat and horizontal surface. Defining as V_x the liquid volume from the leftmost well wall (at $-l$) to x the liquid volume flow rate through an x cross section can be estimated for a cylindrical well as

$$Q = -\frac{dV_x}{dt} = -\frac{d\int_{-l}^{x} [h(t) + \delta(t)]w(x')dx'}{dt}$$
$$= -\frac{x(l^2 - x^2)^{3/2} \delta_{lmax} \pi f \sin(2\pi ft)}{2l^2}$$

It follows that in a cylindrical well the maximum flow rate observed at $x = \pm\frac{1}{2}l$ is given by

$$Q_{max} - \mp\frac{3\sqrt{3}}{32} r^2 \delta_{lmax} \pi f \sin(2\pi ft)$$

corresponding to a cross section average velocity (volume flux) of the form

$$u_{x\,average} = \frac{Q}{A} = \frac{Q}{(h+\delta)w} = \frac{3r\delta_{lmax}\pi f}{32h_0} \sin(2\pi ft)$$
$$= U_0 \sin(2\pi ft)$$

To provide an estimate of the fluid velocity distribution and the associated shear stress the corresponding oscillating wall problem (second Stokes problem [34]) is considered using $U_{x\,average}$ as the forcing wall velocity. With this assumption the velocity distribution within the fluid has the form:

$$u_x(y,t) = U_0 e^{y\sqrt{(\pi f/\nu)}} \sin\left(2\pi ft - y\sqrt{(\pi f/\nu)}\right)$$

The hydrodynamic shear stress at the substrate surface can be estimated as

$$\tau_0 = -\mu \left.\frac{\partial u_x}{\partial y}\right|_{y=0}$$
$$= -\mu \frac{3r\delta_{lmax}(\pi f)^{3/2}}{32h_0\sqrt{\nu}} [\cos(2\pi ft) + \sin(2\pi ft)]$$

Maximum shear corresponds to time instances satisfying $2\pi ft = k\pi + \frac{\pi}{4}$ and is equal to

$$\tau_{0,max} = 0.1326 \frac{\rho\sqrt{\nu} r \delta_{lmax} (\pi f)^{3/2}}{h_0}$$

References

1. O.P. Hamill, B. Martinac, Physiol. Rev. **81**, 685 (2001)
2. G. Apodaca, Am. J. Physiol. Renal Physiol. **282**, F179 (2002)
3. M. Chiquet, Matrix Biol. **18**, 417 (1999). doi:10.1016/S0945-053X(99)00039-6
4. A.J. Putnam, K. Schultz, D.J. Mooney, Am. J. Physiol. Cell Physiol. **280**, C556 (2001)
5. E.H. Burger, J. Klein-Nulend, FASEB J. **13**, S101 (1999)
6. P.G. Ziros, A.P.R. Gil, T. Georgakopoulos, I. Habeos, D. Kletsas, E.K. Basdra, A.G. Papavassiliou, J. Biol. Chem. **277**(26), 23934 (2002). doi:10.1074/jbc.M109881200
7. K.A. Bhatt, E.I. Chang, S.M. Warren, S.E. Lin, N. Bastidas, S. Ghali, J. Surg. Res. **143**(2), 329 (2007)
8. R.A. Jackson, A. Kumarasuriyar, V. Nurcombe, S.M. Cool, J. Cell. Physiol. **209**(3), 894 (2006). doi:10.1002/jcp.20779
9. U. Meyer, M. Terodde, U. Joos, H.P. Wiesmann, Mund Kiefer Gesichtschir. **5**(3), 166 (2001). doi:10.1007/s100060100293
10. L.V. Harter, K.A. Hruska, R.L. Duncan, Endocrinology **136**(2), 528 (1995). doi:10.1210/en.136.2.528
11. Y.Q. Yang, X.T. Li, A.B. Rabie, M.K. Fu, D. Zhang, Front. Biosci. **1**(11), 776 (2006). doi:10.2741/1835
12. J. You, C.E. Yellowley, H.J. Dinahue, Y. Zhang, Q. Chen, C.R. Jacobs, J. Biomech. Eng. **122**(4), 387 (2000). doi:10.1115/1.1287161

13. Y.J. Li, N.N. Batra, L. You, S.C. Meier, I.A. Coe, C.E. Yellowley, C.R. Jacobs, J. Orthop. Res. **22**(6), 1283 (2004). doi:10.1016/j.orthres.2004.04.002
14. N.N. Batra, Y.J. Li, C.E. Yellowley, L. You, A.M. Malone, C.H. Kin, C.R. Jacobs, J. Biomech. **38**(9), 1909 (2005). doi:10.1016/j.jbiomech.2004.08.009
15. J. Klein-Nulend, J. Roelofsen, C.M. Semeins, A.L.J.J. Bronckers, E.H. Burger, J. Cell. Physiol. **170**, 174 (1997). doi:10.1002/(SICI)1097-4652(199702)170:2<174::AID-JCP9>3.0.CO;2-L
16. X.F. Walboomers, W.J. Habraken, B. Feddes, L.C. Winter, J.D. Bumgardner, J.A. Jansen, J. Biomed. Mater. Res. A **69**(1), 131 (2004). doi:10.1002/jbm.a.20127
17. V.I. Sikavitsas, J.S. Temenoff, A.G. Mikos, Biomaterials **22**, 2581 (2001). doi:10.1016/S0142-9612(01)00002-3
18. B. Labat, T. Chepda, J. Frey, J. Rieu, J.L. Aurelle, M. Douet, C. Alexandre, A. Chamson, Biomaterials **21**(12), 1275 (2000). doi:10.1016/S0142-9612(00)00013-2
19. F. Di Palma, A. Chamson, M.H. Lafage-Proust, P. Jouffray, O. Sabido, Peyroche, L. Vico, A. Rattner, Biomaterials **25**(13), 2565 (2004). doi:10.1016/j.biomaterials.2003.09.026
20. T.D. Brown, J. Biomech. **33**, 3 (2000). doi:10.1016/S0021-9290(99)00177-3
21. N. Basso, J.N.M. Heersche, Bone **30**(2), 347 (2002). doi:10.1016/S8756-3282(01)00678-0
22. L.C. Winter, J.A. Gilbert, S.H. Elder, J.D. Bumgardner, Ann. Biomed. Eng. **30**(10), 1242 (2002). doi:10.1114/1.1529195
23. M. Bottlang, M. Simnacher, H. Schmidt, R.A. Brand, L. Claes, Biomed. Tech. (Berl.) **42**, 305 (1997)
24. L.-L. Tang, Y.-L. Wang, J. Pan, S.X. Cai, J. Biomech. **37**, 157 (2004). doi:10.1016/S0021-9290(03)00237-9
25. H.L. Jessop, S.C.F. Rawlinson, A.A. Pitsillides, LE Lanyon, Bone **31**(1), 186 (2002). doi:10.1016/S8756-3282(02)00797-4
26. T.D. Brown, M. Bottlang, Pedersen, A.J. Banes, Am. J. Med. Sci. **316**(3), 162 (1998). doi:10.1097/00000441-199809000-00003
27. D.B. Burr, A.G. Robling, C.H. Turner, Bone **30**, 781 (2002). doi:10.1016/S8756-3282(02)00707-X
28. R.A. Brand, C.M. Stanford, D.P. Nicolella, J. Orthop. Sci. **6**, 295 (2001). doi:10.1007/s007760100051
29. F. Di Palma, M. Douet, C. Boachon, A. Guignandon, S. Peyroche, B. Forest, C. Alexandre, A. Chamson, A. Rattner, Biomaterials **24**(18), 3139 (2003). doi:10.1016/S0142-9612(03)00152-2
30. D.V. Kilpadi, G.N. Raikar, J. Liu, J.E. Lemons, Y. Vohra, J.C. Gregory, J. Biomed. Mater. Res. **40**(4), 646 (1998). doi:10.1002/(SICI)1097-4636(19980615)40:4<646::AID-JBM17>3.0.CO;2-D
31. K.L. Kilpadi, P.L. Chanq, S.L. Bellis, J. Biomed. Mater. Res. **57**(2), 258 (2001). doi:10.1002/1097-4636(200111)57:2<258::AID-JBM1166>3.0.CO;2-R
32. E. Bonnelye, L. Merdad, V. Kung, J.E. Aubin, J. Cell Biol. **153**(5), 971 (2001). doi:10.1083/jcb.153.5.971
33. M.C. Meazzini, C.D. Toma, J.L. Schaffer, M.L. Gray, L.C. Gerstenfeld, J. Orthop. Res. **16**(2), 170 (1998). doi:10.1002/jor.1100160204
34. H. Schlichting, *Gersten K Boundary-Layer Theory* (Springer-Verlag, New York, 2000)
35. F. Di Palma, A. Guiqnandon, A. Chamson, M.H. Lafage-Proust, N. Laroche, S. Peyroche, L. Vico, A. Rattner, Biomaterials **26**(20), 4249 (2005). doi:10.1016/j.biomaterials.2004.10.041
36. M. Lewandowska-Szumiel, K. Sikorski, A. Szummer, Z. Lewandowski, W. Marczynski, J. Biomech. **40**(3), 554 (2007). doi:10.1016/j.jbiomech.2006.02.012
37. D.B. Burr, C. Milgrom, D. Fyhrie, M. Forwood, M. Nyska, A. Finestone, S. Hoshaw, E. Saiag, A. Simkin, Bone **18**, 405 (1996). doi:10.1016/8756-3282(96)00028-2
38. H.M. Frost, Bone Miner. **19**(3), 257 (1992). doi:10.1016/0169-6009(92)90875-E
39. A.E. Goodship, J. Kenwright, J. Bone Joint Surg. Br. **67**(4), 650 (1985)
40. T. Kanno, T. Takahashi, W. Ariyoshi, T. Tsujisawa, M. Haga, T. Nishihara, J. Oral Maxillofac. Surg. **63**, 499 (2005). doi:10.1016/j.joms.2004.07.023
41. M. Koike, H. Shimokawa, Z. Kanno, K. Ohya, K. Soma, J Bone Miner. Metab. **23**, 219 (2005). doi:10.1007/s00774-004-0587-y
42. D. Kaspar, W. Seidl, C. Neidlinger-Wilke, L. Claes, J. Musculoskelet. Neuronal Interact. **1**(2), 161 (2000)
43. D. Kaspar, W. Seidl, C. Neidlinger-Wilke, A. Beck, L. Claes, A. Ignatius, J. Biomech. **35**(7), 873 (2002). doi:10.1016/S0021-9290(02)00058-1
44. P. Ducy, T. Schinke, G. Karsenty, Science **289**(5484), 1501 (2000). doi:10.1126/science.289.5484.1501
45. M. Jagodzinski, M. Drescher, J. Zeichen, S. Hankemeier, C. Krettek, U. Bosch, M. van Griensven, Eur. Cell Mater. **7**, 35 (2004)
46. A.D. Bakker, K. Soejima, J. Klein-Nulend, E.H. Burger, J. Biomech. **34**(5), 671 (2001). doi:10.1016/S0021-9290(00)00231-1
47. S.R. Bannister, C.H. Lohmann, Y. Lin, V.L. Sylvia, D.L. Cochran, D.D. Dean, B.D. Boyan, L. Schwartz, J. Biomed. Mater. Res. **60**, 167 (2002). doi:10.1002/jbm.10037
48. P. Papagerakis, A. Berdal, M. Mesbah, M. Peuchmaur, L. Malaval, J. Nydergger, J. Simmer, M. Macdougall, Bone **30**(2), 377 (2002). doi:10.1016/S8756-3282(01)00683-4
49. I. Owan, D.B. Burr, C.H. Turner, J. Qiu, Y. Tu, J.E. Onyia, R.L. Duncan, Am. J. Physiol. **273**, C810 (1997)
50. C.D. Toma, S. Ashkar, M.L. Gray, J.L. Schaffer, L.C. Gerstenfeld, J. Bone Miner. Res. **12**(10), 1626 (1997). doi:10.1359/jbmr.1997.12.10.1626
51. D. Liu, B.B. Vandahl, S. Birkelund, L.B. Nielsen, B. Melsen, Eur. J. Orthod. **26**(2), 143 (2004). doi:10.1093/ejo/26.2.143
52. M.R. Kreke, W.R. Huckle, A.S. Goldstein, Bone **36**(6), 1047 (2005). doi:10.1016/j.bone.2005.03.008
53. T. Standal, M. Borset, A. Sundan, Exp. Oncol. **26**(3), 179 (2004)
54. J. You, G.C. Reilly, X. Zhen, C.E. Yellowley, Q. Chen, H.J. Donahue, C.R. Jacobs, J. Biol. Chem. **276**(16), 13365 (2001). doi:10.1074/jbc.M009846200
55. R.G. Bacabac, T.H. Smit, M.G. Mullender, S.J. Dijcks, J.J. Van Loon, J. Klein-Nulend, Biochem. Biophys. Res. Commun. **315**(4), 823 (2004). doi:10.1016/j.bbrc.2004.01.138
56. J.G. McGarry, J. Klein-Nulend, P.J. Prendergast, Biochem. Biophys. Res. Commun. **330**(1), 341 (2005). doi:10.1016/j.bbrc.2005.02.175